COUPLED TRANSPORT-CHEMO-MECHANICAL SIMULATION OF CEMENT/AGGREGATE SAMPLES AFFECTED BY DEF AT THE AGGREGATE SCALE. EFFECTS OF PRE-CRACKED INTERFACE AND COMPARISON WITH EXPERIMENTAL DATA

LAMA BRAYSH[*], CÉLINE PELISSOU[*], FREDERIC PERALES[*] AND ADRIEN SOCIÉ[†]

[*] IRS[N] Institut de Radioprotection et de Sûreté Nucléaire, CEA Cadarache, France

[†] CEA, DES, IRESNE, DEC, SESC, F-13108 Saint-Paul-Lez-Durance, France

Key words: Delayed Ettringite Formation (DEF), Reactive transport, Multiphysics modeling, Frictional Cohesive Zone Model

Abstract: Concrete structures are widely used due to their long-term durability and strength; however, they are susceptible to deterioration and fracture once subjected to chemical reactions and/or mechanical stresses. One specific example of this type of degradation is the phenomenon of delayed ettringite formation that can occur under combined environmental conditions and exposure to high temperatures at early age. This often leads to the swelling, micro and macro-cracking and at a later stage the deterioration of massive concrete structures with loss of strength. In this context, the aim of the work is to predict, characterize and monitor the chemical and mechanical behavior of mature concrete affected by DEF pathology at "aggregate scale" using 3D numerical simulations. A composite parallelepiped sample composed of CEM I cement paste bonded to siliceous aggregate have been simulated to perform a qualitative comparison with experimental results ($1\times1\times3$ cm^3 sample dimensions). The chemo-poromechanical model is based on the coupling between a poromechanical model, in the framework of Frictional Cohesive Zone Model for fracture. The initial chemical parameters and mechanical properties of the cement paste have been estimated from the chemical composition of the cementitious mix that was used in the previous experimental work. The effect of the initial degradation at the interface between cement paste and the aggregate have been studied. Our work shows that the initial cracks affect the ettringite precipitation and hence modify the cracking pathology in the sample. These results show good agreement with the crack propagation and swelling evolution in the sample as compared to experimental data.

1 INTRODUCTION

During the lifetime of concrete structures, delayed deformation and chemical reactions can degrade the material and diffusion properties of the concrete materials. Some sources of these delayed stresses might also be internal. For instance, when hydrated concrete experiences high curing temperatures in its early stages, sodium leaching can lead sulfates inside the concrete mix to react with the calcium aluminate present, producing ettringite that forms and precipitates inside the pores of the concrete. This leads to the swelling and to micro and macro cracking that eventually would propagate, increasing swelling and resulting in a loss of mechanical strength and deterioration of the concrete structure. This pathology is known as Delayed Ettringite Formation (DEF). The phenomena and parameters controlling DEF are multiscale and multiphysics, where the concrete microstructure properties impact the swelling behavior [1]. It is thus important to study at the mesoscale the pathology as well as the effect of cracks caused by DEF on concrete.

In this work, we are interested in characterizing and monitoring the chemical

and mechanical behavior of matured concrete affected by Delayed Ettringite Formation. To better understand the local phenomena, 3D numerical simulations of cement/aggregate samples are used to study the ettringite formation at the aggregate scale, within a coupled transport-chemo-poromechanical model [2], in comparison to previous experimental work [3].

2 EXPERIMENTAL SAMPLE

A previous experimental work has been done to study the DEF pathology and identify the location of degradation at the cement paste/aggregate interface [3].

The sample used was a composite parallelopiped sample composed of siliceous aggregates bonded by a Portland cement paste (CEM I 52.5 R, see Table 1 for the chemical composition) of dimensions $1\times1\times3$ cm^3 with a Water/Cement ratio of 0.47. The choice of the cement and the siliceous aggregates was in favor to triggering DEF formation. They also increased the alkali content (which was initially 0.35%) to 1.2% by adding Na_2SO_4 to the cement with a proportion of 6.77 kg/m^3 to increase the kinetics of DEF. Cement paste samples with the same size as composites were used as a reference.

Table 1: Chemical composition of CEM I 52.5 R [3]

Components	Content (%)
K_2O	0.35
SO_3	3.59
Fe_2O_3	3
Al_2O_3	4.15
MgO	1
Na_2O	0.16
Na_2O_{eq}	1.2

The samples underwent a hydrothermal treatment in a climate chamber while maintaining a relative humidity of 95%, by an increase in the temperature by 5°C/hour, from 20°C, before being preserved at 80°C for 2 hours. This step has been done directly after casting into silicone molds. After applying this thermal cycle, the samples were preserved in a distilled water tank at a temperature of 38°C.

The expansion of the samples was tracked using the image correlation technique by a speckle pattern placed on one side of the sample and later following the development of the pathology by taking images of this face each seven days.

This local experimental study [3], gave us the opportunity to compare and validate the chemo-mechanical model developed in [2]. This work will help us to upscale the model and simulate concrete samples affected by DEF.

3 CHEMO-POROMECHANICAL MODEL

The chemo-poromechanical model couples a reactive transport model with a poromechanical model. This model aims to predict the swelling caused by chemical species precipitation and its mechanical consequences, in particular the initiation and propagation of cracks. Fracture analysis is performed using a micromechanical model based on a multibody concept and the Frictional Cohesive Zone Model (FCZM) [2], [4].

3.1 Reactive transport model

The reactive transport model describes the evolution of mineralogy in fractured concrete. For each time step, species transport and geochemical equilibrium are solved sequentially. In this model, the geomaterial is assumed to be fully saturated, and the transport of ions to be driven by the concentration gradient of the species. The transport of the materials follows Fick's law formulated in terms of concentration:

$$\frac{\partial \emptyset C_i^{aq}}{\partial t} = \nabla \cdot \left(D_i \nabla C_i^{aq} \right) + \frac{\partial \emptyset (C_i^{aq})^{\Xi}}{\partial t} \qquad (1)$$

where C_i^{aq} [mol.L^{-1}] and D_i [m^2.s^{-1}] represent the concentration and the effective diffusion coefficient of species i, respectively, and $\emptyset$ denotes the porosity. The term $\frac{\partial \emptyset (C_i^{aq})^{\Xi}}{\partial t}$ acts as a source/sink term, accounting for the creation or consumption of ion i in solution due to chemical reactions [mol.L^{-1}.s^{-1}].

2

In the chemical solver, chemical processes are assumed to be in thermodynamic equilibrium. Electroneutrality is imposed and chemical reactions are assumed to be reversible and instantaneous. We consider the solid, aqueous and sorption reactions.

The chemical model of the DEF takes into account the link between the sulfate sorption and the sodium leaching. The solid reactions are described in the Table 2 and the sorption reactions in the Table 3 [5].

Table 2: Solid reactions used for DEF simulations [5].

Chemical equations	$log_{10}(K)$
Portlandite $\Leftrightarrow Ca^{2+} + 2OH^{-}$	-5.19
Katoite $\Leftrightarrow 2Al(OH)_4^{-} + 3Ca^{2+} + 4OH^{-}$	-20.5
Ettringite$\Leftrightarrow 2Al(OH)_4^{-} + 6Ca^{2+} + 3SO_4^{2-} + 4OH^{-} + 26H_2O$	-44.9

Table 3: Sorption reactions used for DEF simulations [5].

Chemical equations	$log_{10}(K)$
$\equiv Si-OH + Ca^{2+} + OH^{-} + SO_4^{2-} \Leftrightarrow \equiv Si-OCaSO_4^{-} + H_2O$	7.3
$\equiv Si-OH + Na^{+} + OH^{-} + SO_4^{2-} \Leftrightarrow \equiv Si-ONaSO_4^{2-} + H_2O$	5.8

3.2 Poromechanical model

The poromechanical model is composed of two parts: one which handles the volumetric behavior, i.e. the poromechanics of safe materials, and another which handles the surface behavior responsible for the cracks. The volumetric behavior part aims to estimate the mechanical and diffusive parameters and to identify the expansion caused by significant solid precipitation in a porous medium described by an isotropic elastic poromechanical model [2], [6]. This resolution is based on the Biot formulation where the pressure is influenced by the volume fraction of the primary precipitated solid and the strain tensor [2], [5]:

$$\sigma = \mathbb{C}: \varepsilon - bPI$$

$$P = N \langle \varphi_s - \langle \varphi_s^0 + b\, tr\, \varepsilon \rangle_+ \rangle_+ \qquad (2)$$

where σ is the Cauchy stress tensor [Pa], $\mathbb{C}$ is the fourth-order stiffness tensor [Pa], ε is the linearized strain tensor, P is the pore pressure

[Pa], I is the identity second-order tensor, b is the Biot coefficient assuming overall isotropy [−], N is the Biot skeleton modulus [Pa], and $\langle x \rangle = (x + |x|) / 2$ are the Macaulay brackets. φ_s is the main precipitated solid (here, the ettringite) and $\varphi_s^0 \in [0,1]$ is a model parameter that represents the quantity of initial pores to be filled with solid precipitates to induce swelling. We use the subscript s to define the variable associated with the main solid phases. This pressure will eventually lead to stress and local swelling.

For the initiation and propagation of cracks and post-fracture phenomena, we use the Frictional Cohesive Zone Model (FCZM) which relates the cohesive stress R^{adh} [Pa.m^{-1}] to the displacement jump of the crack lips [u] [m] by a damageable surface second order stiffness tensor $K(\beta)$ and considers the post fracture pressure such that:

$$R^{adh} = K(\beta).\, [u] \qquad (3)$$

The value of β represents the adhesion of the interface where the value of 1 corresponds to a sound interface and $\beta = 0$ demonstrates a totally broken interface. The cracks that are initiated and propagated in the material alter the diffusion of the chemical solution [5].

3.3 Chemo-poromechanical modeling

The coupling strategy follows a Sequential Iterative Approach and we compute at each time step the reactive transport through a fixed point (species transport and geochemistry), then the poromechanics of the solid phases. A small time step is mandatory for the computation of the Frictional Cohesive Zone Model and the diffusive time step is scaled [5]. These physical models have been implemented in XPER code (eXtented cohesive zone models and PERiodic homogenization) [4], which will be used in this study.

4 NUMERICAL ESTIMATIONS OF INPUT PARAMETERS

The cement paste is considered mature. So, an initialization step is required to estimate the microstructure and the initial concentrations on one hand, and the mechanical parameters

by analytical homogenization on the other hand [7]. The only value that is approximated without using the model, is the volume fraction φ_s^0 which is normally fitted or estimated. In this work the value of φ_s^0 is assumed to be 10^{-3}. A detailed explanation on the procedure used in this part is well explained in the following studies [2], [5], [7], [8].

4.1 Chemical approximation

The aim of this approximation is to estimate the chemical composition of the mature cement paste, based on that used for the composite samples in experiments. The electroneutrality is imposed upon the hydroxide ion and the chemical solver includes two steps. The first one is the hydration reactions of the cement which occurs upon the addition of water, and the second step is to consider the sorption reactions. Table 4 presents the initial concentrations obtained of each chemical component.

Table 4: The estimated initial chemical parameters.

Chemical component	Concentration (mol.L^{-1})
Ca^{2+}	5.7836×10^{-3}
OH^-	6.4953×10^{-2}
SO_4^{2-}	4.7243×10^{-5}
Al^{3+}	1.5762×10^{-5}
Na^+	5.3496×10^{-2}
$Si-ONaSO_4^{2-}$	0.1125
$Si-OCaSO_4^-$	0.1979
Portlandite	20.5864
Katoite	1.4671
Ettringite	0.7239
CSH	16.5369

4.2 Mechanical approximation

The homogenization scheme is used to approximate the macroscopic elastic parameters follows the Mori-Tanaka scheme applied for mature cement [9]. It is the same for the mechanical and diffusive properties. This scheme considers spherical inclusions embedded in an infinite matrix with interactions between inclusions. At the cement paste scale, the continuous reference matrix is the C-S-H matrix, and the inclusions including

hydrates, capillary porosity and anhydrous cement in our case, are randomly distributed within the paste. The homogenization results obtained are summed up in Table 5. And the initial cohesive parameters are described in Table 6 in reference to [5].

Table 5: The initial mechanical parameters used in the simulations. The initial value of φ_s^0 is an approximate value.

D [m^2.s^{-1}]	ν	E[GPa]	b	N[MPa]	φ_s^0
3.82×10^{-12}	0.25	19.16	0.27	175×10^9	10^{-3}

Table 6: The initial cohesive parameters used [5].

σ_I [Pa]	σ_{II} [Pa]	ω_I [J.m^{-2}]	ω_{II} [J.m^{-2}]
4.6×10^7	46×10^7	20	200

5 APPLICATIONS

Using XPER code [4], we simulate a composite sample ($1\times1\times3$ cm^3) composed of a cement paste matrix connected to an aggregate (see Figure 1). The matrix phase is composed of a CEM I cement paste based on the mix described in the experimental work (see Table 1). The temperature is constant T = 25°C. The sample is discretized into 29236 tetrahedral meshes and the mesh size used is 1mm.
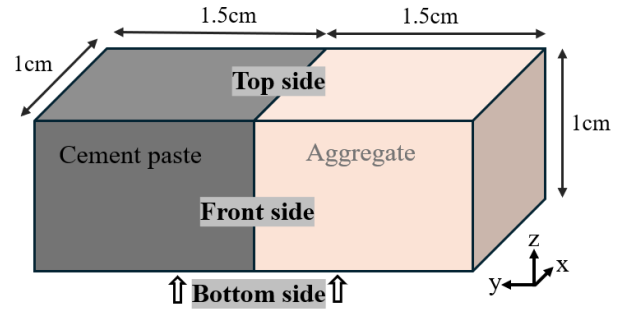

Figure 1: The numerical sample prepared, composed of cement paste and the aggregate. The top, front and bottom sides represent the predefined sides of the sample.

The initial chemical properties (Table 4) and the initial mechanical parameters (Table 5 and Table 6) were estimated based on the experimental data. The sample is placed along its longest (the bottom side defined in Figure 1), and we assume a no-diffusive flux at the boundaries considering that it was immersed in water in experiments. The mechanical time

step dt is 5×10^{-8} seconds and the diffusion time step is 1 hour.

5.1 Effect of interface cracking on the DEF evolution

For a composite sample, the interface between the cement paste and the aggregate, also called ITZ, can alter the chemical transport and hence the diffusion and precipitation of ettringite. This would eventually lead to a change in the pathology of cracks. We are interested in the effect of the interface on the DEF pathology through an initial crack, where different values of initial adhesion are considered (from initially total sound interface towards a totally cracked interface). In our model, the initial crack at the interface is monitored by modifying β value in equation (3).

β represents the initial cracks at the interface between cement paste and aggregate; this value is bounded between zero and one. The value of zero indicates a totally cracked interface, where we have an initial gap between both phases and the value of one indicates a totally sound interface without any cracks between both phases. We consider three different values of beta (0, 0.6 and 1), with the same initial chemical and mechanical parameters. For each, we compute its respective initial displacement value from the cohesive zone law. Note that a specific value of β indicates this constant value all along the interface. These values are summed up in Table 7.

Table 7: The chosen values of initial cracking β with their corrresponding values of initial displacement u_0.

β	u_0 (m)
0	6.87×10^{-7}
0.6	2.27×10^{-7}
1	0.0

In our simulations, cracks initiate due to ettringite precipitation and then propagate in the sample, causing at a later stage the deterioration of the interface and creating gaps between the paste and aggregate which favors the precipitation of solids in this space.

In Figure 2, we show the ettringite precipitation (top image) and the resulting cracks that formed in the top side of the cement paste (bottom image), for a β value of 0.6. The cracks form close to the boundary as a result of the precipitated ettringite which is also affected by the boundary conditions. This concave shape of ettringite causes a higher stress parallel to the boundary and hence this shape of cracks is formed on the top side of the sample.
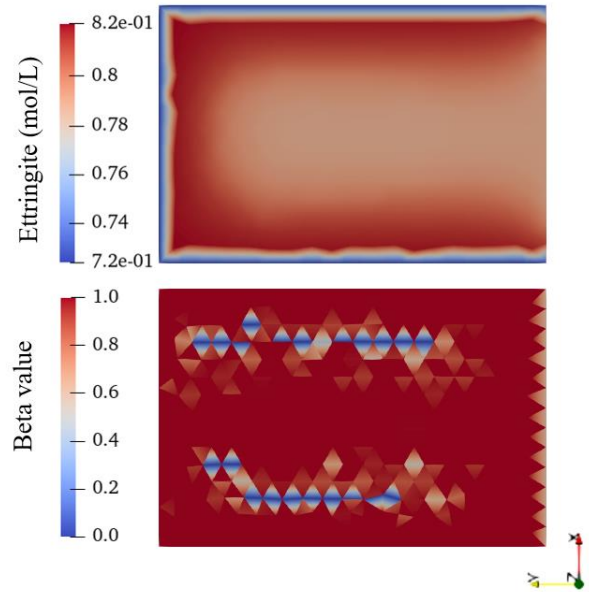

Figure 2: Ettringite precipitation on the bottom side of the sample and the resulting crack path on the top side for β = 0.6 after 4.5 days.

The effect of ettringite precipitation creates such cracks on the top side of the sample, however, a cracked interface would lead to a change in the pathology once these initial cracks widen and propagate through the sample. This is mainly because the cracks alter the diffusion and hence the precipitation. The presence of cracks at the interface between the cement paste and the aggregate will cause in addition to the boundary conditions effect, a local precipitation of ettringite at the interface. As a result, cracks initially present will expand and different pathology may appear depending on the interface. To demonstrate the effect of the cracked interface, we compare the DEF pathology at the same time of three samples of β equal to 0, 0.6 and 1 as shown in Figure 3.
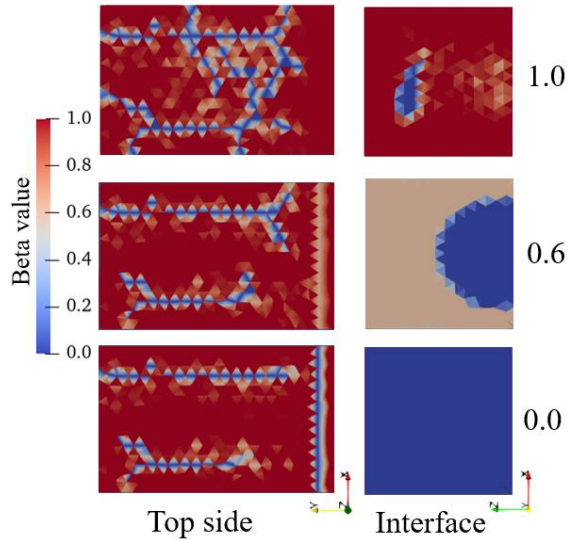
Figure 3: Effect of initial interface cracking on the DEF pathology (in blue the damage i.e. β < 0.4) after nearly 12 days.

Figure 3 shows the pathology of the three samples of different initial interface cracking value β on the top face of the sample (images on the left) and at the interface (images on the right) after nearly 12 days. For β = 0, the interface is totally cracked. For β = 0.6, we can see that the cracks initiate where part of the interface is totally broken (the blue colored part) and the rest is partially cracked. For β = 1, part of the interface remains totally sound while a small part begins to crack. As a result of this difference at the interface level, the cracks path on the top face varies between these samples.

This is due to the difference in the stress caused by the precipitated ettringite and the different locations of the initial cracks. We can see that the sound sample has more cracks on the top than the samples with cracked and partially cracked interfaces. This can be interpreted by the different local expansion which lead to a local stress between these samples. When there are no initial cracks at the interface, less ettringite will be localized near the interface. In that way, there will be more precipitation near the boundary causing more localized stress and hence more stress.

Figure 4 presents a cross section in the yz plane in the middle of the sample of initial β = 0.6. In this figure, we can see the ettringite precipitation near the boundaries and near the

interface and therefore the induced cracks, which demonstrates the effect of the precipitated ettringite on the crack formation. Furthermore, this figure highlights the capacity of the model to tackle complex chemo-mechanical phenomena. Initially ettringite precipitated at the boundaries induces cracks by differential stress (swelling in the attack area). Then the sodium leaching is localized and accelerated inside the cracks, which induces ettringite near cracks.
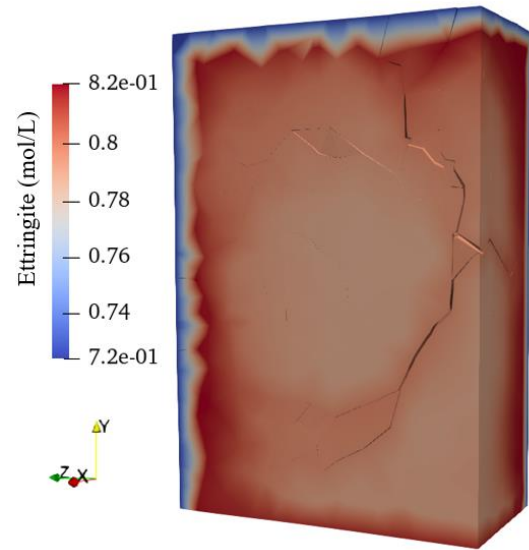

Figure 4: Cross section of the sample after 12 days with initial β=0.6 at the interface. The color bar represents the concentration of ettringite, and the crack width in this figure is scaled by a value 3.

5.2 Comparison with experiments

The pathology obtained in our simulation (for β = 0.6) was compared to the pathology that was obtained in experiments in Figure 5. The top image in the figure presents one sample taken from the experimental work [1] and the image below demonstrates the pathology obtained numerically with initial β = 0.6 at the interface.

We can clearly notice the lines parallel to the boundary in experiment and a similar result is obtained in our simulation. This shows that using our model we were able to obtain a similar crack path to experiments.
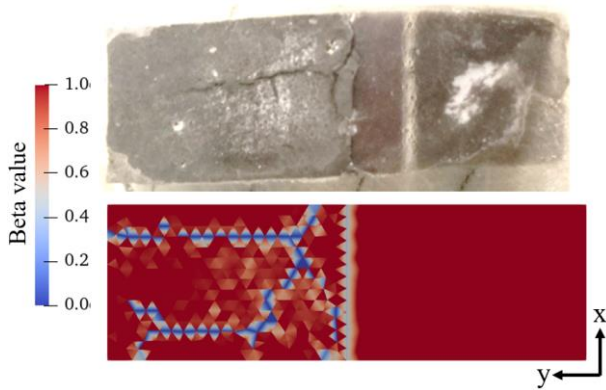
Figure 5: A top side image of the composite sample from experiment (on top) and from simulations (at the bottom) with initial $\beta = 0.6$. On the left side of the sample, is the cement, and on the right, the aggregate.

6 CONCLUSION

This study is based on numerical modelling of the behavior of a composite sample composed of cement paste bonded to an aggregate by an interface with varied initial cracks. The crack propagation is followed for each of these cases, and we demonstrate through this study the effect of initial cracks on the pathology due to internal sulfate reactions. In comparison to experimental results, our numerical results, mainly the crack shape are qualitatively in accordance with experimental data. This work can be used to upscale the model to the macro scale and simulate concrete samples affected by DEF.

REFERENCES

[1] M. Al Shamaa, S. Lavaud, L. Divet, J. B. Colliat, G. Nahas, and J. M. Torrenti, « Influence of limestone filler and of the size of the aggregates on DEF », *Cement and Concrete Composites*, vol. 71, p. 175-180, 2016.

[2] A. Socié, F. Dubois, Y. Monerie, and F. Perales, « Multibody approach for reactive transport modeling in discontinuous-heterogeneous porous media », *Comput Geosci*, vol. 25, nᵒ 5, p. 1473-1491, 2021.

[3] M. Jebli, F. Jamin, C. Pelissou, E. Lhopital, and M. S. E. Youssoufi, « Characterization of the expansion due to the delayed ettringite formation at the cement paste-aggregate interface », *Construction and Building Materials*, vol. 289, p. 122979, 2021.

[4] F. Perales, F. Dubois, Y. Monerie, B. Piar, and L. Stainier, « A NonSmooth Contact Dynamics-based multi-domain solver: Code coupling (Xper) and application to fracture », *European Journal of Computational Mechanics*, vol. 19, p. 389-417, 2010.

[5] A. Socié, F. Dubois, Y. Monerie, M. Neji, and F. Perales, « Simulation of internal and external sulfate attacks of concrete with a generic reactive transport-poromechanical model », *European Journal of Environmental and Civil Engineering*, vol. 27, nᵒ 12, p. 3679-3706, 2023.

[6] O. Coussy, *Poromechanics*, 2nd ed. Chichester, England ; Hoboken, NJ: Wiley, 2004.

[7] A. Socié, Y. Monerie, and F. Péralès, « Effects of the microstructural uncertainties on the poroelastic and the diffusive properties of mortar », *Journal of Theoretical, Computational and Applied Mechanics*, p. 8849, 2022.

[8] J. Pouya, M. Neji, L. De Windt, F. Péralès, A. Socié, and J. Corvisier, « Investigating chemical and cracking processes in cement paste exposed to a low external sulfate attack with emphasis on the contribution of gypsum », *Construction and Building Materials*, vol. 413, p. 134845, 2024.

[9] T. Mori and K. Tanaka, « Average stress in matrix and average elastic energy of materials with misfitting inclusions », *Acta Metallurgica*, vol. 21, nᵒ 5, p. 571-574, 1973.